Kime, M. J., & Moore, P. B. (1983) *FEBS Lett. 155*, 199-203.
Kime, M. J., Ratcliffe, R. G., Moore, P. B., & Williams, R. J. P. (1981) *Eur. J. Biochem. 116*, 269-276.
Lightfoot, D. R., Wong, K. L., Kearns, D. R., Reid, B. R., & Shulman, R. G. (1973) *J. Mol. Biol. 78*, 71-89.
Luoma, G. A., & Marshall, A. G. (1978) *Proc. Natl. Acad. Sci. U.S.A. 75*, 4901-4905.
Luoma, G. A., Burns, P. D., Bruce, R. E., & Marshall, A. G. (1980) *Biochemistry 19*, 5456-5462.
Madison, J. T. (1968) *Annu. Rev. Biochem. 37*, 131-148.
Monier, R. (1974) in *Ribosomes* (Nomura, M., Tissieres, A., & Lengyel, P., Eds.) pp 141-168, Cold Spring Harbor Laboratory, Cold Spring Harbor, NY.
Osterberg, R., Sjoberg, B., & Garrett, R. A. (1976) *Eur. J. Biochem. 68*, 481-487.
Pieler, T., & Erdmann, V. A. (1982) *Proc. Natl. Acad. Sci. U.S.A. 79*, 4599-4603.
Raacke, I. D. (1968) *Biochem. Biophys. Res. Commun. 31*, 528-533.
Reid, B. R. (1981) *Annu. Rev. Biochem. 50*, 969-996.
Reid, B. R., & Hurd, R. E. (1977) *Acc. Chem. Res. 10*, 396-402.
Reid, B. R., McCollum, L., Abeiro, N. S., Abbate, J., & Hurd, R. E. (1979) *Biochemistry 18*, 3996-4005.
Rosset, R., & Monier, R. (1963) *Biochim. Biophys. Acta 68*, 653-656.
Roy, S., & Redfield, A. G. (1981) *Nucleic Acids Res. 9*, 7073-7083.
Salemink, P. J. M., Raue, H. A., Heerschap, A., Planta, R. J., & Hilbers, C. W. (1981) *Biochemistry 20*, 265-272.
Sanchez, V., Redfield, A. G., Johnston, P. D., & Tropp, J. (1980) *Proc. Natl. Acad. Sci. U.S.A. 77*, 5659-5662.
Schimmel, P. R., & Redfield, A. G. (1980) *Annu. Rev. Biophys. Bioeng. 9*, 191-221.
Studnicka, G. M., Eisenberg, F. A., & Lake, J. A. (1981) *Nucleic Acids Res. 9*, 1885-1904.
Weidner, H., Yuan, R., & Crothers, D. M. (1977) *Nature (London) 266*, 193-194.
Wong, Y. P., Kearns, D. R., Reid, B. R., & Shulman, R. G. (1972) *J. Mol. Biol. 72*, 741-749.
Zimmermann, R. A. (1980) in *Ribosomes Structure, Function & Genetics* (Chambliss, G., Craven, G. R., Davies, J., Davis, K., Kahan, L., & Nomura, M., Eds.) pp 135-170, University Park Press, Baltimore, MD.

Nuclear Overhauser Experiments at 500 MHz on the Downfield Proton Spectra of 5S Ribonucleic Acid and Its Complex with Ribosomal Protein L25†

M. J. Kime and P. B. Moore*

ABSTRACT: The downfield (9-15 ppm) proton spectrum of *Escherichia coli* 5S RNA has been examined at 500 MHz by using nuclear Overhauser methods. The data confirm the existence of the terminal and procaryotic loop helices within the molecule [Fox, G. E., & Woese, C. R. (1975) *Nature (London) 256*, 505-506]. Very little stable, double-helical structure is detectable in the third loop of the molecule, the one comprising bases 12-68. The downfield spectrum of 5S RNA is perturbed in a highly specific manner upon addition of protein L25 to the system. The changes seen strongly suggest that the binding site for L25 on 5S RNA includes the procaryotic loop helix, but not the terminal stem helix. Similar complexes formed between L25 and the 5S RNA fragment consisting of bases 1-11, 69-87, and 89-120 show exactly the same spectral alterations. A number of downfield resonances appear in the spectra of these complexes which have no counterparts in the free RNA, suggesting the stabilization of new RNA structures by the protein. There are some indications of protein-nucleic acid nuclear Overhauser effects.

Proton nuclear magnetic resonance (NMR) techniques have been used to study the structure and properties of RNAs for over a decade [for review see Kearns & Shulman (1974); Kearns, 1976, 1977; Reid & Hurd, 1977; Schimmel & Redfield, 1980; Reid, 1981]. The tRNAs have been the subject of much of this work, but 5S RNA, the next larger abundant RNA species, has also received attention (Wong et al., 1972; Kearns & Wong, 1974; Burns et al., 1980; Luoma et al., 1980; Salemink et al., 1981). The portion of a nucleic acid proton spectrum of particular interest is the downfield region (9-15 ppm) where hydrogen-bonded base pair imino protons resonate. Powerful methods have been developed lately for assigning the downfield resonances of small nucleic acids based on the nuclear Overhauser effect (NOE) (Johnston & Redfield, 1978, 1981; Sanchez et al., 1980; Roy & Redfield, 1981; Hare & Reid, 1982a,b; Roy et al., 1982). It is clear that the problem of the assignment of the spectra of tRNAs will soon be solved in several cases.

Recently we have begun applying the NMR methods which work so well for tRNAs to the interpretation of the downfield proton spectrum of 5S RNA and its complexes with ribosomal proteins. It has been shown that the large 5S RNA fragment derived from the whole molecule by limited ribonuclease A (RNase A) digestion (Douthwaite et al., 1979) has a secondary, and probably a tertiary, structure similar to that of

† From the Department of Chemistry, Yale University, New Haven, Connecticut 06511. *Received January 3, 1983; revised manuscript received March 4, 1983.* This research was supported by a grant (to P.B.M.) from the National Institutes of Health (AI-09167). M.J.K. is a NATO/SERC postdoctoral fellow. NMR spectroscopy was done at the Northeast Regional NMR Facility which is supported by the National Science Foundation (CHE-7916210).

0006-2960/83/0422-2622$01.50/0

the same sequences in intact 5S RNA (Kime & Moore, 1983a). NOE methods have produced data consistent with the presence of the two helical stems predicted to lie within the fragment sequence (bases 1–11, 69–87, and 89–120) by the Fox–Woese (1975) model for the parent, 5S RNA secondary structure (Kime & Moore, 1983b).

This paper reports the results of a series of observations made on the downfield spectra of *Escherichia coli* 5S RNA, its complex with ribosomal protein L25 [see Garrett et al. (1981)], and the corresponding L25–fragment complex (Douthwaite et al., 1979). The presence of the helical segments found in the fragment is confirmed in the parent molecule. While many resonances can be observed in the intact 5S RNA molecule which are not present in the fragment, which is only half the size of the whole molecule, relatively few of these resonances can presently be assigned to helical structures by NOE techniques. The constant loop (bases 12–68) portion of 5S RNA, the part missing from the fragment, seems to be less stable than the terminal stem and procaryotic loop portions.

When L25 is added to 5S RNA, the downfield spectrum is perturbed in a manner which is exactly duplicated in the fragment–L25 complex, again confirming the structural similarity of the two RNA molecules. This result is taken to indicate that the L25 binding site is localized in the fragment region of the 5S RNA. NOE experiments carried out on the fragment–L25 complex permit the identification of the RNA resonances perturbed by protein binding. These changes are most easily rationalized on the assumption that the procaryotic loop helix is part of the L25 binding site. A number of new downfield resonances appear in the complex, suggestive of new, protein-stabilized structures in the RNA. Moreover, presaturation of upfield protein methyl resonances gives NOEs to a resonance whose chemical shift is well downfield of any protein exchangeable resonances. This NOE is indicative of an intimate interaction between L25 and 5S RNA.

Materials and Methods

5S RNA. "Ribosomal" 5S RNA was prepared from 50S subunits or 70S ribosomes from *E. coli* MRE600 by standard methods (Kime & Moore, 1982). It was also obtained from bulk, low molecular weight RNA from *E. coli B* (Plenum Scientific Research, Hackensack, NJ) by chromatography on Sephacryl S-200 in 0.15 M NaCl, 1% methanol, and 0.1 M sodium acetate, pH 5.0, at 23 °C (Kime & Moore, 1983b).

For many experiments a 5S RNA called "rrnB" 5S RNA was used. This RNA was made from *E. coli* HB101/pKK5-1, a strain which carries the rrnB 5S cistron on PBR322 (Brosius et al., 1981). In this case, following growth under overproducing conditions, a ribosome-free supernatant was prepared by centrifugation. The supernatant was phenol extracted and the RNA purified as for *E. coli* B 5S RNA (Kime & Moore, 1983b).

5S RNA Fragment. The preparation of fragment has been described elsewhere (Kime & Moore, 1983a). 5S RNA at 1 mg/mL was exposed to 10 μg/mL RNase A at 0 °C for 45 min at pH 7.8. Following digestion RNase was removed by phenol extraction and the fragment purified by chromatography on Sephadex G-75.

L25 and L25–5S Complexes. Ribosomal protein L25 was prepared as described previously (Kime et al., 1981; Kime & Moore, 1982). The protein, in urea, was dialyzed into 0.1 M KCl, 4 mM $MgCl_2$, and 5 mM cacodylic acid, pH 7.2, the buffer used both for complex formation and subsequent spectroscopy. Its concentration was estimated from its extinction coefficient at 276 nm by using 0.38 as the absorbance of a 1 mg/mL solution of this protein. 5S RNA or 5S fragment solutions were prepared in the same buffer. Concentrations were estimated from absorbance at 260 nm by using 847 OD/mL as equivalent to a 1 mM solution of 5S RNA (Osterberg et al., 1976) and 437 OD/mL as the extinction coefficient of a 1 mM solution of fragment. (The latter extinction coefficient assumes that the hyperchromicities of fragment and 5S RNA are identical; there are 62 bases in the fragment and 120 in the intact parent molecule.)

Complexes were formed by adding L25 to solutions of RNA at concentrations around 0.1 mM. The resulting mixtures were concentrated by ultrafiltration using Amicon YM-5 filters to obtain samples whose RNA concentrations were around 1.0 mM. Solvents for NMR contained 5% D_2O to permit the operation of the spectrometer lock.

NMR Spectroscopy. This was performed as previously described (Kime & Moore, 1983a). All data were collected at 303 K unless otherwise noted. Techniques for interpreting NOE data from the downfield region of RNA spectra have been worked out by Redfield and his co-workers. They hinge on the fact that the NOE is a short-range effect in nucleic acids, usually limited to 4 Å or less. Thus when a hydrogen-bonded base, imino proton is presaturated, the NOEs seen are generally limited to the next-nearest neighbor protons. These will include the hydrogen-bonded imino protons of the base pairs immediately above and below the base pair whose proton is presaturated (Johnston & Redfield, 1981). There will also be transfer to nearby amino protons, but these give broad NOEs in the aromatic region around 8 ppm.

Presaturation of an AU base pair imino proton, either of the Watson–Crick or reverse Hoogsteen type, gives a sharp, strong NOE in the aromatic region in addition to the NOEs in the downfield region to its nearest neighbors (Sanchez et al., 1980). The proton seen is either a C2 proton (Watson–Crick) or a C8 proton (reverse Hoogsteen) on the A of the AU pair. This upfield NOE distinguishes an AU downfield resonance from a GC downfield resonance.

GU wobble base pairs also can be recognized (Johnston & Redfield, 1978; Roy & Redfield, 1981). In this case there will be a pair of imino resonances around 11 ppm which will give strong, intrabase NOEs to each other as well as weaker, interbase NOEs to other resonances in the downfield region.

The use of NOE experiments for assigning the resonances in RNA helices has been illustrated elegantly by Hare & Reid (1982a,b) and by Roy et al. (1982).

Results

Intact 5S RNA. To facilitate discussion of the spectrum of 5S RNA it is useful to have a system for naming resonances consistent with the one devised for the spectrum of its fragment (Kime & Moore, 1983b). Every resonance in the fragment spectrum has a correspondent at virtually the same chemical shift in the spectrum of the parent molecule. We give those 5S RNA resonances the same designation they have been given in the fragment spectrum, namely, upper case letters.

The "extra" features in the spectrum of intact 5S RNA can best be recognized by subtracting the fragment spectrum from that of the whole molecule. The result of such a manipulation is shown in Figure 1 where the spectrum of the fragment (Figure 1b), suitably line broadened to match the line widths of resonances in the whole molecule spectrum, on average, is subtracted from the spectrum of the whole molecule (Figure 1a) to give a difference spectrum (Figure 1c). The peaks in the difference spectrum are designated with lower case letters. Figure 2 shows a resolution-enhanced fragment spectrum with its resonances lettered (Figure 2a) and a spectrum of intact

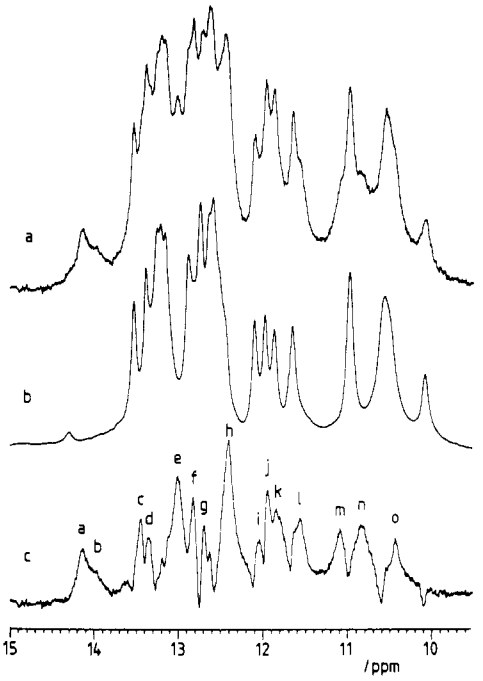

FIGURE 1: Comparison of the spectra of intact 5S RNA and its RNase A resistant fragment. The spectra of both species were accumulated at concentrations of about 1.0 mM in 0.1 M KCl, 4 mM $MgCl_2$, and 5 mM cacodylic acid, pH 7.2 at 303 K. A 5-s pulse cycle time was used to ensure full relaxation of the macromolecular protons. (Spectrum a) Ribosomal 5S RNA; (spectrum b) ribosomal 5S RNA fragment, line broadened 13.5 Hz; (spectrum c) spectrum a minus spectrum b.

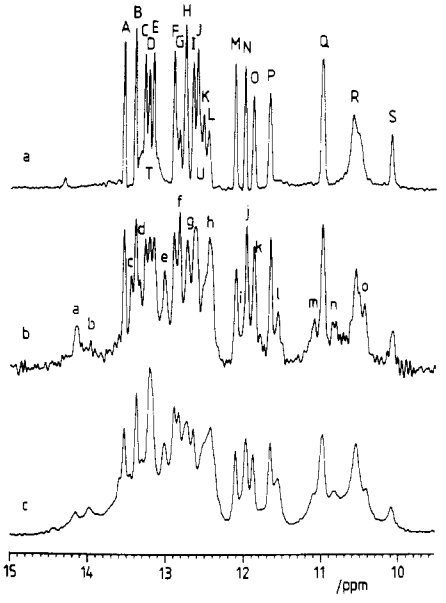

FIGURE 2: Resolution-enhanced spectra of 5S RNA and fragment. Fully relaxed spectra were accumulated and resolution enhanced by Gaussian multiplication: (a) ribosomal 5S RNA fragment, (b) ribosomal 5S RNA, and (c) rrnB 5S RNA. The spectra used for (a) and (b) are the same as those shown in Figure 1. The peak designations are shown. In spectrum b only the peaks unique to 5S RNA are indicated.

5S RNA, also resolution enhanced, with the positions of the "new" resonances indicated (Figure 2b).

The samples whose spectra are shown in Figures 1, 2a, and 2b are ribosomal 5S RNA and the fragment made therefrom. In much of the work discussed below, rrnB 5S RNA was used, the spectrum of which differs somewhat from that of ribosomal 5S RNA. Figure 2c shows the rrnB 5S RNA spectrum. The

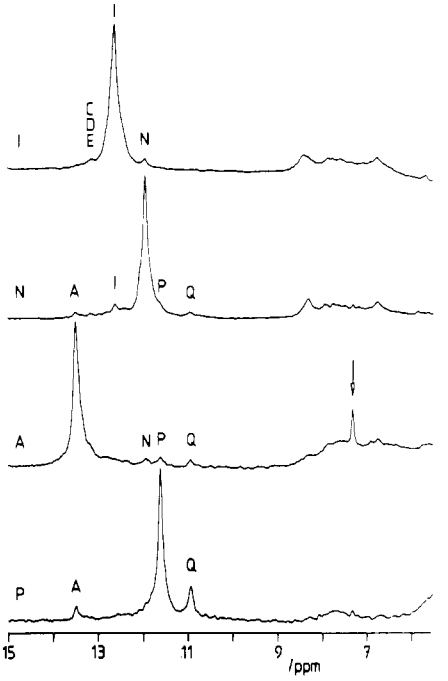

FIGURE 3: NOEs given by rrnB 5S RNA at 37 °C. Four NOE difference spectra are shown. Each is designated by the name of the peak presaturated, which is always the strongest peak in the difference spectrum. The weaker resonances induced by NOE are labeled for identification. The arrow at about 7.2 ppm in spectrum "A" designates a strong upfield NOE.

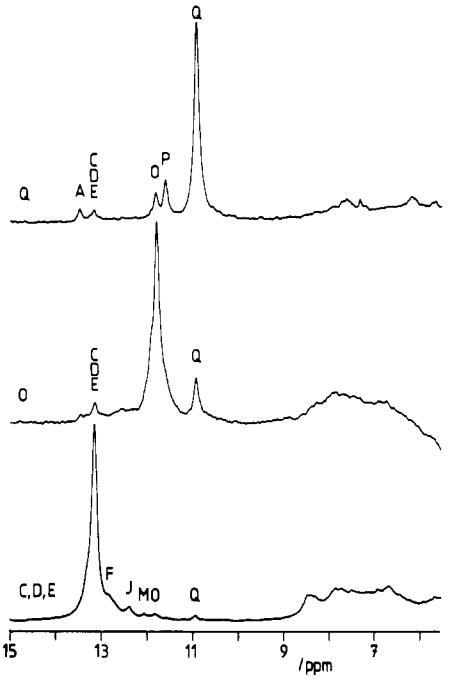

FIGURE 4: Further NOEs given by rrnB 5S RNA (see legend for Figure 3).

main differences between the two spectra are that resonance C has moved upfield in rrnB to lie on top of D and E and J has shifted upfield so it lies on top of K and L.

NOEs on 5S RNA. All the downfield resonances in the intact rrnB 5S molecule have been examined for NOEs at 37 °C, pH 7.2, in 0.1 M KCl and 2 mM $MgCl_2$. The 5S RNA spectrum under these conditions appears identical with the spectrum in Figure 2c but has the significant advantage of slightly narrower resonances and so better resolution. One of the helical progressions in the 5S spectrum is illustrated

starting with resonance I (Figure 3) and ending with resonances (C, D, E) which overlap (Figure 4).

When I is presaturated (Figure 3), a strong NOE is seen to N, a weaker NOE is seen to (C, D, E), which overlap in the parent spectrum, and no strong, sharp NOE appears in the aromatic region. The (C, D, E) NOE contribution is due to overlap of resonance I with resonance H. Resonance I is a GC base pair which ends a helical segment whose neighboring base pair is represented by N. Presaturation of N (Figure 3) brings up I, as expected, as well as A, P, and Q. The effects to A, P, and Q are understood when A is presaturated (Figure 3). Presaturation of A elicits N, P, and Q. Resonance A has a strong NOE to a sharp upfield resonance, indicating it represents an AU base pair. Apparently saturation is being transferred efficiently from A or N through the chain of base pairs represented by resonances N, A, P, and Q. When P is presaturated (Figure 3), an extremely strong NOE to Q is seen and a weaker NOE to A. The strong P–Q relationship suggests that P and Q are imino protons in the same base pair, presumably a GU base pair. Presaturation of Q gives P and A, as expected, but also O and (C, D, E) (Figure 4). When O is presaturated, Q and (C, D, E) appear, suggesting that O and Q are GU imino protons which relate by NOE to a GC base pair whose imino proton resonates at position (C, D, E). Presaturation of the (C, D, E) overlapped resonance (Figure 4) brings up O and Q, but also J, F, and M (see below). Thus two helical segments are recognized, I, N, A, P, and Q, resonances whose properties suggest a helical segment of the following sequence, $(GC)_2(AU)(GU)$, and (C, D, E), O, and Q corresponding to (GC)(GU). The fragment spectrum has NOEs linking I, N, A, P, and Q and D, O, and Q. The former set of resonances corresponds well with the helical structure suggested for the procaryotic loop of 5S by Fox & Woese (1975) and Kime & Moore (1983b).

A similar progression starting with J reveals the sequence J, (C, D, E), F, B, M, (C, D, E), H in the intact molecule (data not shown) which corresponds to the fragment NOE progression J, C, F, B, M, E, H assigned earlier to a helical stack of the form $(GC)_3(AU)(GC)_3$, which fits in the terminal stem of the molecule (Kime & Moore, 1983b). Of the resonances upfield of Q which have correspondents in the fragment, only S has an NOE in the whole molecule, and it is to H, again reminiscent of the fragment. Thus the main secondary structure features found in the fragment spectrum by NOE are found also in the whole molecule, as the similarity of their spectra with respect to chemical shift suggested would be true (Kime & Moore, 1983a).

The surprise in these experiments lies in the paucity of NOEs in the intact molecule spectrum beyond those found in the fragment. The resonances saturated to elicit the NOEs already described, in many cases, overlap nonfragment, whole molecule resonances, yet no new NOEs were seen. Moreover, resonances like a, b, c, and e which are resolved in the 5S spectrum gave no detectable NOEs when irradiated.

The cases where nonfragment NOEs were detected generally involved considerable experimental difficulties; Figure 5 is an example. In Figure 5, resonance P is presaturated, and NOEs are detected to Q and A as usual. When the frequency of the preirradiation is shifted upfield to presaturate l, a shoulder downfield of Q at the position of resonance m is seen as well as a feature at d. Irradiation at m brings up O, P, and A due to overlap with Q, but the peak at P has a definite upfield shoulder and the downfield resonance, d, is also apparent. Shift of the radiation frequency to the center of resonance Q results in the loss of these "extra" features.

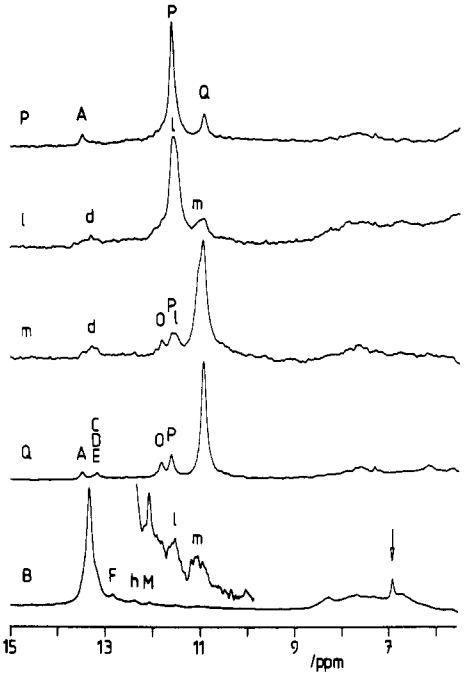

FIGURE 5: Nonfragment NOEs in rrnB 5S RNA (see legend for Figure 3).

Spectrum B shows that presaturation near resonance d elicits (barely) the expected NOEs to l and m. A further NOE can be detected from h to d, suggesting the existence of a helical stem $(GC)_2(GU)$. The nonfragment NOEs are difficult to detect because nonfragment resonances typically appear broader, are often of reduced (hence, nonintegral) intensity, and commonly overlap with the sharper fragment-related resonances.

Reduction of the temperature at which NOE experiments were done was attempted with 5S RNA to reduce imino proton exchange rates in the constant loop, in hopes of enhancing the NOEs seen. While there were some new effects detected, the 5S RNA spectrum broadens substantially as temperature drops, probably due in part to aggregation (Osterberg et al., 1976). With *E. coli* 5S RNA one appears to be confronted with either "high"-resolution spectra and many NOEs undetectable because of rapid RNA–solvent exchange at high temperature (37 °C) or bad spectra with intrinsically better NOEs which are effectively undetectable due to line width at lower temperature (below 25 °C). Further progress is unlikely on this system under these conditions.

Complexes with L25. Protein L25 binds both to 5S RNA and to fragment (Douthwaite et al., 1979). Figure 6 shows spectra of protein L25 (Figure 6a), of a mixture of L25 and ribosomal fragment at a stoichiometry of about 0.5:1 (Figure 6b), and of fragment, free of protein (Figure 6c). These spectra extend from roughly 5.5 to 15 ppm and give an overall view of the downfield effects which accompany the formation of the nucleoprotein complex. Figure 7 concentrates on the region between 9.5 and 15 ppm. Figure 7b shows the spectrum of a stoichiometric complex of L25 and 5S RNA at a concentration of 0.5 mM. Figure 7a is the spectrum of protein free 5S RNA, while spectrum c is spectrum b minus spectrum a. Negative features in the difference correspond to resonances in the free RNA molecule which have changed chemical shift position or disappeared in the complex. Positive features represent resonances in the complex for which there are no counterparts at the same chemical shift position in the free molecule. It is clear that the presence of the protein perturbs many, but by no means all, resonances in the downfield region.

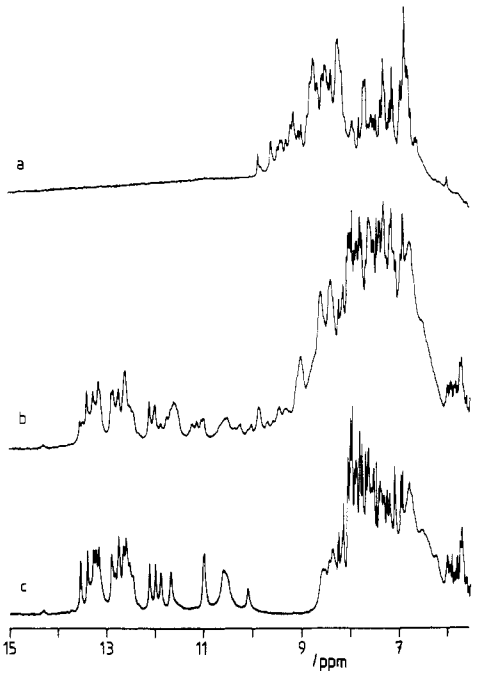

FIGURE 6: Spectra from 6 to 15 ppm of fragment, L25, and fragment–L25 complex. Free L25 (a), free ribosomal fragment (c), and L25–fragment complex (about 0.5 mol of protein/1.0 mol of RNA) (b). No line broadening was applied to the free induction decays.

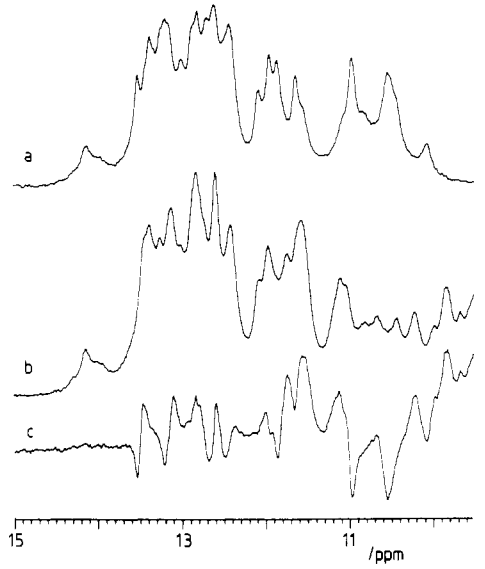

FIGURE 7: Effect of L25 binding on the downfield spectrum of ribosomal 5S RNA. Samples of 5S RNA and L25–5S RNA complex were prepared as given under Materials and Methods. The 5-s cycle time spectra were accumulated and are shown here plotted with identical line broadening. (a) Free ribosomal 5S RNA; (b) the complex of 5S RNA and L25 in about 1:1 molar ratio; (c) spectrum b minus spectrum a.

In addition there are new resonances appearing upfield of resonance S just downfield of where the most downfield of the free protein NH resonances fall (see Figure 6). Figure 8 compares four difference spectra of the kind shown in Figure 7c. The upper three (Figure 8a–c) are from three separate L25–fragment complex samples and two fragment samples (i.e., one fragment sample served as RNA control for both spectra b and c) having L25 to fragment ratios of roughly 0.5:1 (a), 0.9:1 (b), and 1:1 (c). Figure 8d is the whole molecule difference spectrum from Figure 7. It should be emphasized that all seven spectra used to construct Figure 8 are absolute intensity spectra accumulated with 5-s pulse cycle times. It

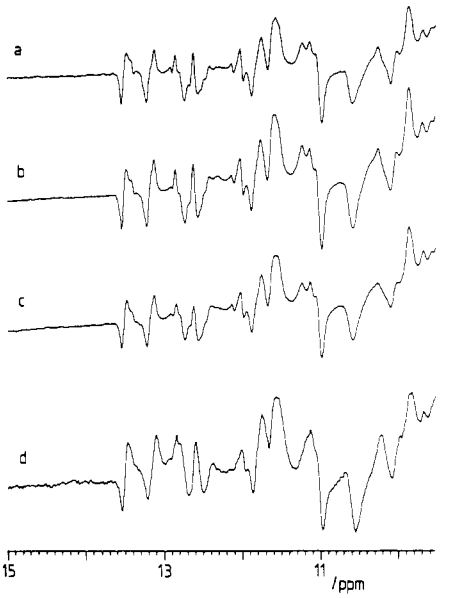

FIGURE 8: Binding difference spectra compared. Several differences (complex – RNA) are shown. All were obtained as described in Figure 7, but fragment spectra were line broadened by 9 Hz more than L25–fragment complex spectra before taking differences. (Spectrum a) L25–fragment complex at a protein to RNA ratio of about 0.5:1. (Spectrum b) L25–fragment complex at a protein to RNA ratio of about 0.9:1. (Spectrum c) L25–fragment complex at a protein to RNA ratio of about 1:1. (Spectrum d) L25–5S RNA complex at a 1:1 ratio (same as Figure 7c).

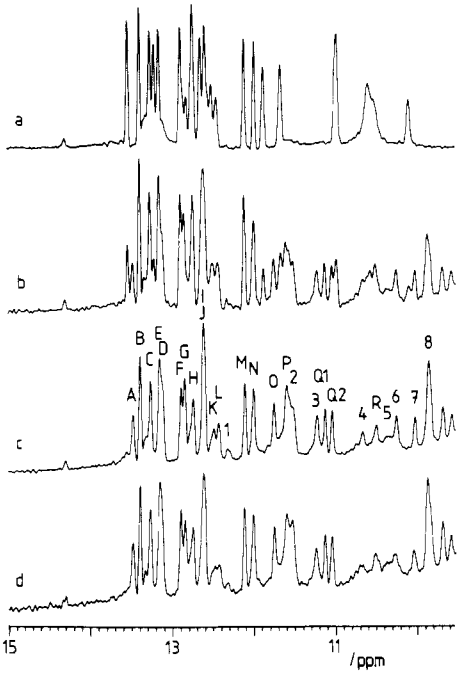

FIGURE 9: Titration of fragment with L25. The fragment–L25 complex spectra which contributed to Figure 8 are shown. (Spectrum a) Free fragment; (spectrum b) fragment complex at 0.5:1; (spectrum c) fragment complex at 0.9:1; (spectrum d) fragment complex at 1:1.

is clear that whatever happens when L25 binds to 5S RNA also occurs when that protein binds to fragment. Accordingly, from the NMR standpoint, it is satisfactory to study the L25–5S interaction using the fragment complex. The L25 binding site appears to be wholly contained in the fragment component of 5S RNA.

Figure 9 shows the fragment–protein complex titration series which gave rise to Figure 8a–c. All spectra are shown in resolution-enhanced form to aid identification of the spectral

changes which take place upon protein binding, many of which are clearly apparent. Resonances A, D, and I have each moved about 0.1 ppm upfield, leading to the superposition of D and E and I and J. Resonance N shifts about 0.05 ppm downfield while O has moved more than 0.1 ppm upfield. In the complex there are at least two resonances at about the chemical shift of P, and Q has been "replaced" by three resolved resonances. The P resonances are upfield of the original P position, and the Q resonances are all downfield. In addition, the relative intensities of G and H appear to alter, and K and L are less intense in the complex than in free fragment.

Clearly the resonances most strongly affected by protein binding are the group I, N, A, P, Q already known to be associated because they belong to the $(GC)_2(AU)(GU)$ helix in the procaryotic loop stem. The fact that D, O, and Q which constitute a short (GU)(GC) sequence also change suggests that there is an association between these two helical regions and that resonances D, O, and Q also originate in the procaryotic loop. This assignment is consistent with the double-helical stem $(GC)_2(AU)(GU)_2(GC)$, predicted by the Fox–Woese 5S RNA secondary structure model. Virtually nothing happens to resonances in the terminal stem group, J, C, F, B, M, E, H, with the possible exception of H.

Fragment Complex NOEs. The spectrum of the almost fully titrated complex, 9c, is labeled for further reference. Resonances which correspond to unassociated fragment resonances are designated with upper case letters, as usual. Where a resonance of that kind splits during complex formation, the products are designated X1, X2, ... There are several resonances in the spectrum of the complex which have no obvious counterparts in the free RNA. These are designated by numbers.

Resonances were assigned by using NOE experiments done at both 30 and 20 °C. Some experiments were also performed at 10 °C. At both higher temperatures a progression of resonances (I, J), C, F, B, M, (D, E), H was easily identified, indicating that the helix assigned as $(GC)_3(AU)(GC)_3$ is still intact even though some overlapping of resonances occurs in the complex which would confuse the issue were the free fragment spectrum unknown. The (I, J), N, A, P, Q progression, on the other hand, is interrupted in the complex. The N to A NOE, easily shown in free fragment, has virtually vanished, particularly at low temperatures. (This change again supports the view that the I, N, A, P, Q helix is being affected by L25 binding.) The (D, E), O, and Q sequence anticipated from both fragment and whole molecule studies is intact, and at low temperature, the (C, E), P, and R relationship, (GC)(GU), can also be detected (data not shown). The (C, E), P, and R resonances have identical chemical shift positions in both the isolated fragment and the L25 complex at 10 °C, as far as can be determined. This reinforces the view that of the two (GU)(GC) segments detected in the fragment, the one whose resonances are D, O, and Q is the one more likely to be the continuation of the procaryotic loop stem.

The Q resonance related to P is Q2, the upfield member of the split Q pair. Q1 is connected to O in the (D, E), O, Q progression. The apparent doubling (at least) of the P resonance and tripling of the Q resonance are due to the appearance of resonances in the complex with no obvious counterparts in the free molecule, resonances 2 and 3.

Among the numbered (hence new) resonances, several NOEs can be detected. These are listed in Table I. The new downfield resonances, which are only detected in protein–nucleic acid complex spectra, are difficult to assign: NOEs do not reveal new long progressions of resonances (as for RNA helices). Moreover, there is the additional problem of deciding what these new resonances represent: they could be RNA protons shielded from the solvent by virtue of interactions connected with protein binding, they could be protein protons ring current shifted far downfield under the influence of the RNA bases, or they could represent hydrogen bonds involved in the linking of RNA to protein. In any case, all these resonances represent exchangeable protons: in 100% D_2O solvents the most downfield proton resonances of otherwise identical samples occur at chemical shifts upfield of 9 ppm. Many of the resonances upfield of Q, the last easily recognizable RNA resonance in the complex, have NOEs to resonances in the hydrogen-bonded imino proton region.

NOEs to Protein. Presaturation of some of the new resonances in the complex spectrum appears to produce effects on

Table I: NOEs Involving New Resonances in the Fragment–L25 Complex[a]

resonance	NOEs (comments)	reverse NOE	protein NOE
1	3	yes	no
2	8 (not at low temp)	no	uncertain
3	1 (not at low temp)	yes	no
4	none at room temp		probable
5	none		yes
6	I, 3 (weak)	yes (I), no (3)	no
7	G	yes	uncertain
8	I	yes	yes
upfield of 8	none		yes

[a] Listed in this table are the results of NOE experiments on numbered resonances within the complex spectrum (see Figure 8). The first column is the resonance presaturated. The second gives the identity of the NOE(s) seen and any comments. The third column reports whether an NOE in the reverse direction has been seen. The final column indicates whether a protein spin-diffusion NOE is seen upon presaturation of the resonance in question.

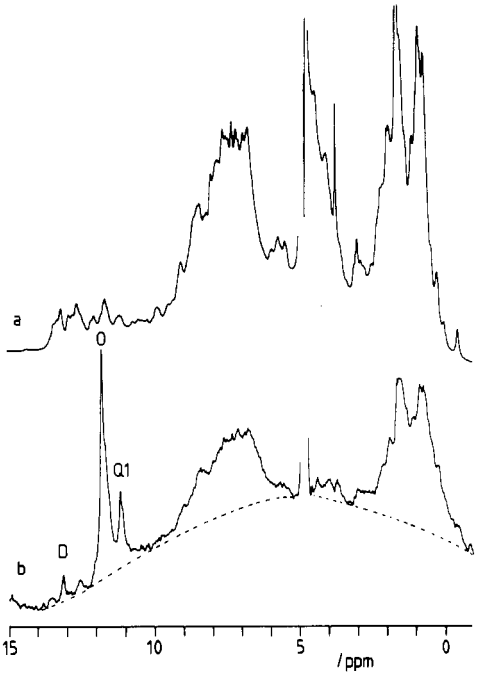

FIGURE 10: Upfield NOEs. The L25–5S RNA fragment complex sample used for this experiment had a protein to RNA ratio of 0.9:1. Resonance O was presaturated. Spectrum a is the off-resonance spectrum used to calculate the NOE difference spectrum, shown here for reference. Spectrum b is the NOE difference. A plausible base line is sketched in. The data were measured at 293 K. Note the chemical shift scale and that, for convenience of presentation, the region upfield of water is shown inverted.

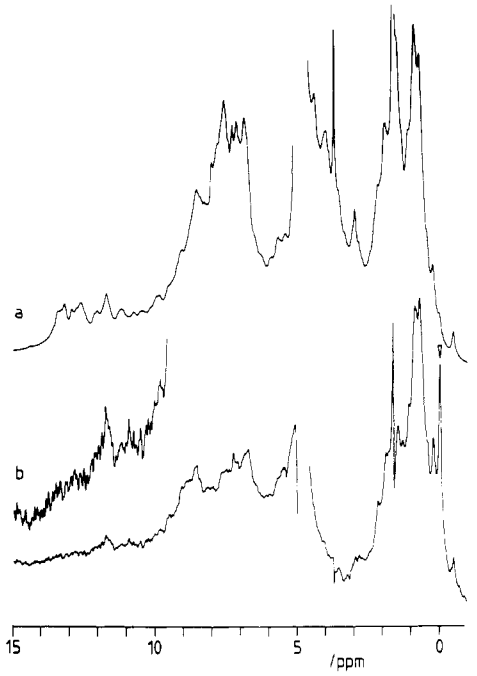

FIGURE 11: Protein to RNA NOEs. The same sample used for the experiment described in Figure 10 was again employed, this time at 283 K. Resonance M2, marked with an arrow in spectrum b, was presaturated. Spectrum a is the off-resonance spectrum shown for reference. Spectrum b is the NOE difference. The region upfield of water is shown inverted.

the protein spectrum upfield of H_2O. All complex NOEs were examined for these effects. There are no NOEs to protein from any of the resonances downfield of O, i.e., resonances A–N, and l. As shown in Figure 10, on the other hand, there is a striking effect observed when O is presaturated. The irradiation is, perhaps, surprisingly selective (but note that both spectra were line broadened to effectively increase line width at half-height by 16 Hz). Selectivity is indicated by the absence of an NOE to A which would have been detected if the nearest resonance to O, that is, P, had been saturated. The difference quality is shown to be excellent by the absence of major spikes where the sharp, intense dioxan chemical shift standard and cacodylate buffer resonances occur. The difference spectrum, however, has a significant protein contribution. This would be even more apparent but for the spectral power characteristics of the observation pulse sequence regime used (Materials and Methods), which excites resonances that are close to H_2O less strongly than it does the downfield imino proton resonances. Presaturation of either of the two most upfield methyl resonances in L25 (M1 and M2; Kime et al., 1981) induces an effect at either O or P (exactly which of these is difficult to specify at this stage) (Figure 11).

Table I records the correlation between the numbered resonances presaturated and this type of protein NOE. Resonances numbered above 8 show NOEs to protein, and to nothing downfield (until, presumably, one is sufficiently upfield to irradiate RNA amino or pyrimidine C5 protons). It is likely that these are protein amide protons. Even in the absence of the RNA there are protein resonances in this part of the spectrum (Figure 6).

Discussion

In many respects the NOE results on intact 5S RNA are disappointing. When one compares Figure 1c, the constant loop and tertiary structure spectrum, with the secondary structure of the standard Fox–Woese model for 5S RNA in the corresponding sequence, bases 12–68, the situation looks extraordinarily hopeful. Resonances a and b, by analogy with tRNA experience, are likely to represent tertiary interactions. Resonances c and d are well positioned to be AU resonances, and two such base pairs are predicted in the standard model. Among resonances j, k, l, m, and n one can easily imagine finding four resonances for the two GU base pairs required. On first glance it appears the entire Fox–Woese structure is there. Yet upon carrying out NOE experiments one comes up with no evidence that c and d are AUs and only one $(GU)(GC)_2$ sequence, a small harvest indeed. Since the resonances are clearly there, and large scale base pairing in unstacked arrays most improbable, it seems to us that rapid exchange of hydrogen-bonded protons with solvent is likely to be obliterating the NOEs which otherwise would be anticipated if, as we have shown for other parts of the molecule, Fox-Woese were essentially correct. The corollary of this hypothesis, which is subject to test, is that the secondary structure in the constant loop must be less stable than in the terminal stem and the procaryotic loop. Indeed this fact may account for the observation that it is the constant loop which digests first when 5S RNA is exposed to RNase.

The conclusion that the constant stem is more flexible than the rest of the 5S molecule does not contradict the finding of Marshall & Smith (1980), based on $^{19}F\{^1H\}$ NOEs, that 5S RNA is a rigid molecule. In their experiment, "rigid" implies a rotational correlation time greater than 10 ns. Indeed without such a correlation time, the negative NOEs reported above would not have been seen in 5S RNA. The flexibility referred to here is flexibility sufficient to permit exchange of hydrogen-bonded imino protons at rates sufficient to inhibit the observation of NOEs involving those protons, rates of the order of 10 Hz or faster.

Perhaps the most striking observation reported above is the identity of the spectral perturbations seen downfield upon binding L25 to 5S RNA and to 5S fragment. A small amount of line broadening accompanies complex formation in the case of the fragment; it is much less noticeable with the intact 5S molecule. The similarity of the alterations seen for the two RNAs confirms their underlying similarity of structure and permits the study of the complex in the fragment system.

The changes seen downfield of Q on complex formation are easily summarized; resonances I, N, A, P, Q and D, O, Q all change chemical shift. There are three new resonances evident: 1, which is weak, and 2 and 3, which are quite strong. Finally resonances H, K, and L lose intensity while resonance G appears to gain. Upfield of Q, there are massive changes. Resonance S and components of R in the fragment spectrum disappear and are replaced by a complex series of resonances, the most upfield of which are certainly protein NH resonances.

By no means can all these alterations be interpreted in detail at this point, but there is a simple hypothesis capable of explaining many of them, in general terms: that protein L25 binds to 5S RNA at a site which includes the procaryotic loop stem and in the process perturbs (but does not destroy) the structure of that stem. The same assignment of the L25 binding site has been made by others in the past on the basis of chemical evidence [see Douthwaite et al. (1982) and references therein] but has not been universally accepted [see Pieler & Erdmann (1982)].

This hypothesis readily accounts for the chemical shift changes of resonances A, I, N, P, and Q which belong to the procaryotic loop stem. It also can explain the change in efficiency of NOEs from N to other resonances upon protein binding. The fact that D, O, and Q also alter is consistent

with the view tha the (GU)(GC) helix they represent also belongs to the procaryotic loop. This suggests that they should be assigned to bases 79 and 80 paired with bases 96 and 97. (NOEs which bridge from I, N, A, P, Q to D, O, Q, however, have not been observed.) The absence of any change in the chemical shift positions of the (C, E), P, and R resonances upon complex formation is evidence that this (GC)(GU) is not the continuation of the procaryotic loop. They may well be the (GU)(GC) continuation predicted for the terminal stem helix (although, again, NOEs which bridge from either P or R to the previously assigned ends of the terminal helix have not been detected).

There is reason to believe that the binding of L25 to 5S RNA brings L25 protons into close proximity with nucleotide bases. The most striking indication of this assertion we presently have is the NOE seen linking resonance O to protein. In addition presaturation of several of the resonances in the downfield region of the complex produced NOE difference spectra which resembled protein spectra. The fact that the entire protein spectrum is affected rather than single resonances suggests extensive cross-saturation within the protein L25 when it is bound to fragment in the complex, i.e., "spin diffusion" (Kalk & Berendsen, 1976). Spin diffusion does not occur in the free protein; specific NOEs have been obtained with it (Kime et al., 1981). Nor is a corresponding spin-diffusion effect observed for the RNA (either isolated or in the complex). (In passing we note that in the case of isolated RNA it is possible to induce a negative NOE which strongly affects all or most of the nucleic acid resonances. This is accomplished by saturation of the poorly resolved ribose CH's. Presaturation of any of the base aromatic protons, however, only produces a localized NOE. Thus the effect is not analogous to the protein spin-diffusion phenomenon in the complex. Presumably this mainly reflects a lower proton density in the RNA moiety of the complex as compared with the bound protein.) The assignments of the downfield resonances which, upon presaturation, gave rise to the nonspecific protein NOEs are of great interest. Some of these resonances are probably protein amide resonances, but others could very well be protons involved in hydrogen bonds linking the RNA to the protein. Obviously a great deal of work will be required to test the assignments and interpretations made here and to complete the task of understanding the spectra shown. The richness of the spectra, however, strongly suggests that these efforts will be rewarded by a substantial improvement in our understanding of this nucleoprotein interaction.

Acknowledgments

We thank Betty Rennie and Grace Sun for their able technical assistance.

References

Brosius, J., Dull, T. J., Sleeter, D. D., & Noller, H. F. (1981) *J. Mol. Biol. 148*, 107–127.

Burns, P. D., Luoma, G. A., & Marshall, A. G. (1980) *Biochem. Biophys. Res. Commun. 96*, 805–811.

Douthwaite, S., Garrett, R. A., Wagner, R., & Feunteun, J. (1979) *Nucleic Acids Res. 6*, 2453–2470.

Douthwaite, S., Christensen, A., & Garrett, R. A. (1982) *Biochemistry 21*, 2313–2320.

Fox, G. E., & Woese, C. R. (1975) *Nature (London) 256*, 505–506.

Garrett, R. A., Douthwaite, S., & Noller, H. F. (1981) *Trends Biochem. Sci. (Pers. Ed.) 6*, 137–139.

Hare, D. R., & Reid, B. R. (1982a) *Biochemistry 21*, 1835–1842.

Hare, D. R., & Reid, B. R. (1982b) *Biochemistry 21*, 5129–5135.

Johnston, P. D., & Redfield, A. G. (1978) *Nucleic Acids Res. 4*, 3599–3615.

Johnston, P. D., & Redfield, A. G. (1981) *Biochemistry 20*, 1147–1156.

Kalk, A., & Berendsen, H. J. C. (1976) *J. Magn. Reson. 24*, 343–366.

Kearns, D. R. (1976) *Prog. Nucleic Acid Res. Mol. Biol. 18*, 91–149.

Kearns, D. R. (1977) *Annu. Rev. Biophys. Bioeng. 6*, 477–523.

Kearns, D. R., & Shulman, R. G. (1974) *Acc. Chem. Res. 7*, 33–39.

Kearns, D. R., & Wong, Y. P. (1974) *J. Mol. Biol. 87*, 755–774.

Kime, M. J., & Moore, P. B. (1982) *Nucleic Acids. Res. 10*, 4973–4983.

Kime, M. J., & Moore, P. B. (1983a) *FEBS Lett. 153*, 199–203.

Kime, M. J., & Moore, P. B. (1983b) *Biochemistry* (preceding paper in this issue).

Kime, M. J., Ratcliffe, R. G., Moore, P. B., & Williams, R. J. P. (1981) *Eur. J. Biochem. 116*, 269–276.

Luoma, G. A., Burns, P. D., Bruce, R. E., & Marshall, R. G. (1980) *Biochemistry 19*, 5456–5462.

Marshall, A. G., & Smith, J. L. (1980) *Biochemistry 19*, 5955–5959.

Osterberg, R., Sjoberg, B., & Garrett, R. A. (1976) *Eur. J. Biochem. 68*, 481–487.

Pieler, T., & Erdmann, V. A. (1982) *Proc. Natl. Acad. Sci. U.S.A. 79*, 4599–4603.

Reid, B. R. (1981) *Annu. Rev. Biochem. 50*, 969–996.

Reid, B. R., & Hurd, R. E. (1977) *Acc. Chem. Res. 10*, 396–402.

Roy, S., & Redfield, A. G. (1981) *Nucleic Acids Res. 9*, 7073–7083.

Roy, S., Papastavros, M. Z., & Redfield, A. G. (1982) *Biochemistry 21*, 6081–6088.

Salemink, P. J. M., Raue, H. A., Heerschop, A., Pleuta, R. J., & Hilbers, C. W. (1981) *Biochemistry 20*, 265–272.

Sanchez, V., Redfield, A. G., Johnston, P. D., & Tropp, J. (1980) *Proc. Natl. Acad. Sci. U.S.A. 77*, 5659–5662.

Schimmel, P. R., & Redfield, A. G. (1980) *Annu. Rev. Biophys. Bioeng. 9*, 181–221.

Wong, Y. P., Kearns, D. R., Reid, B. R., & Shulman, R. G. (1972) *J. Mol. Biol. 72*, 741–749.